Aust. J. Phys., 1989, **42**, 365–77

Cathode Region of a Steady-state Townsend Discharge in Nitrogen

L. J. Kelly, M. J. Brennan[A] *and A. B. Wedding*[B]

School of Physical Sciences, Flinders University of South Australia,
Bedford Park, S.A. 5042, Australia.
[A] Present address: Research School of Physical Sciences,
Australian National University, G.P.O. Box 4,
Canberra, A.C.T. 2601, Australia.
[B] Present address: Department of Physics,
University of Western Australia,
Nedlands, W.A. 6009, Australia.

Abstract

The photon flux technique has been used to study the cathode region of a steady-state Townsend discharge. Spatial variations in the radiation emitted from the $C^3\Pi_u$ and $B^2\Sigma_u^+$ states of molecular nitrogen were detected in the vicinity of the cathode for $E/N = 331$ and 555 Td. In particular, the second positive emission at 337·1 nm is similar to the Holst–Oosterhuis layers observed in rare gas discharges. Monte Carlo simulations describe qualitatively the experimental results. However, modification of the assumed cross sections is required to improve quantitative agreement between simulation and experiment.

1. Introduction

In steady-state Townsend discharges the behaviour of the electron stream is described by constant transport and rate parameters for positions remote from the electrodes. This region, where the normalised energy distribution for all electrons at a given position has reached a steady state, may be defined as a region of equilibrium. In this hydrodynamic regime the energy distribution function depends on both E/N and spatial gradients in the electron concentration (Wedding and Kelly 1989), but is independent of source conditions. In the proximity of the anode and cathode of the discharge, regions of non-equilibrium exist where the hydrodynamic model is not applicable.

The general features of the different regions of a gas discharge have been outlined elsewhere (Blevin 1985). It is the purpose of this paper to consider in more detail the cathode non-equilibrium region of a steady-state Townsend discharge in molecular nitrogen, a region characterised by spatial variations in the electron energy distribution. The Holst–Oosterhuis (1921) luminous layers observed in rare gas discharges (see also Druyvesteyn 1932; Fletcher 1985) provide a striking example of such phenomena. Electrons leaving the cathode gain energy from the field as they move through the drift tube and suffer elastic or inelastic collisions with the gas particles. The main features of the luminous layers in rare gases arise because electrons moving under the influence of the electric field lose only a small amount of energy by recoil in elastic collisions until they reach the threshold of an electronic excitation level.

0004-9506/89/040365$03.00

Inelastic collisions result in a loss of energy by the electron equivalent to the excitation threshold and the emission of radiation as the atom is de-excited. The process is repeated each time electrons gain enough energy from the field to excite the atoms. Provided that the thresholds of the electronic states are closely grouped then a series of inelastic collisions will produce the observed luminous layers and periodic spatial variations in the electron mean energy.

The cathode region in molecular gases is, in general, much more complex than that in atomic gases due to the large number of rotational, vibrational and electronic excitations possible. As a consequence of the large number of energy loss channels, the phenomena observed in the atomic gases may not occur in a molecular gas. Boeuf and Marode (1984) have reported Monte Carlo simulation results for discharges in the highly attaching gas sulfur hexafluoride SF_6, which indicate that large spatial variations in the electron mean energy and attachment rate occur. We note that their model of SF_6 is similar to the inert gases in that the threshold for excitation of the electronic level was well separated (9·7 eV) from the ground state. The present paper reports an experimental study of the cathode region in molecular nitrogen which has a large number of electronic excitation levels whose thresholds are distributed over a wide energy range. The results of a study by Jelenkovic and Phelps (1987) of the light emission from a self-sustained nitrogen discharge are complicated by the presence of electron emission from regions near the cathode edge and the possibility of wall charges. Coupled with the experimental investigation, a detailed Monte Carlo simulation of the discharge, designed to mimic the experimental conditions, was carried out.

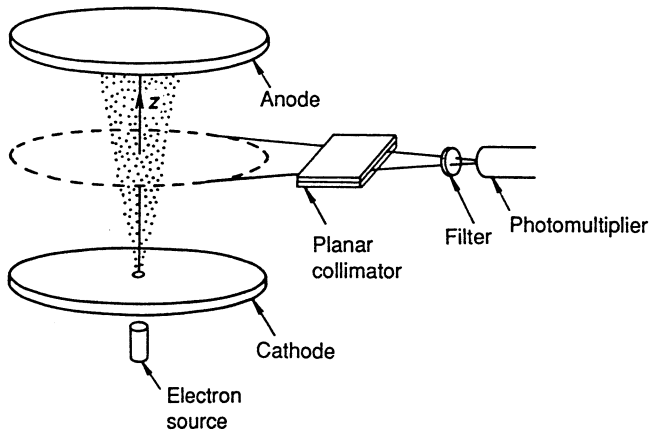

Fig. 1. Schematic diagram of the drift space and planar collimator detection system.

2. Experimental Investigation

The experimental apparatus used in the investigation of the cathode region has been described elsewhere (Wedding *et al.* 1985). The only modification to this apparatus has been an improvement in the design of the planar collimator which detects photons in the plane of the discharge at a given axial position *z*. A schematic diagram of the experimental arrangement for photon detection

is shown in Fig. 1. The present collimator consists of two parallel plates, each 9 cm long and 6 cm wide, separated by precision shims. This design is superior to that of Wedding *et al.* (1985) as deep wells milled into the surface of the plates minimise the possibility of internal photon reflections. The light output from the cathode region of the discharge was thus measured with a spatial resolution at the centre of the drift tube of 0·8 mm (FWHM).

In the present work the cathode–anode separation was held constant at 3·6 cm and a guard ring (i.d. = 11 cm, thickness = 1·6 mm) was positioned midway between the two electrodes (diameter = 15 cm) to maintain electric field uniformity. The inside of the vacuum chamber, electrodes, guard ring and planar collimator were coated with colloidal graphite to further reduce photon reflections. The electron source was an indirectly heated oxide coated cathode, positioned 1 mm behind a 1 mm diameter aperture in the cathode of the drift space. Gas pressures were sufficiently low [0·12–0·14 Torr (1 Torr ≡ 133·332 Pa)] to ensure that very few electrons would inelastically collide before entering the drift region. With the aforementioned pressures and electrode separation the applied gap voltage was sufficiently remote from the breakdown voltage that the contribution from cathode-produced secondary electrons to the overall discharge current was negligible. The discharge current to the anode was used in a feedback circuit to control the thermal emission from the oxide cathode source (Wedding *et al.* 1985). With this arrangement typical discharge currents of the order of 100 nA could be maintained to within ±0·1%.

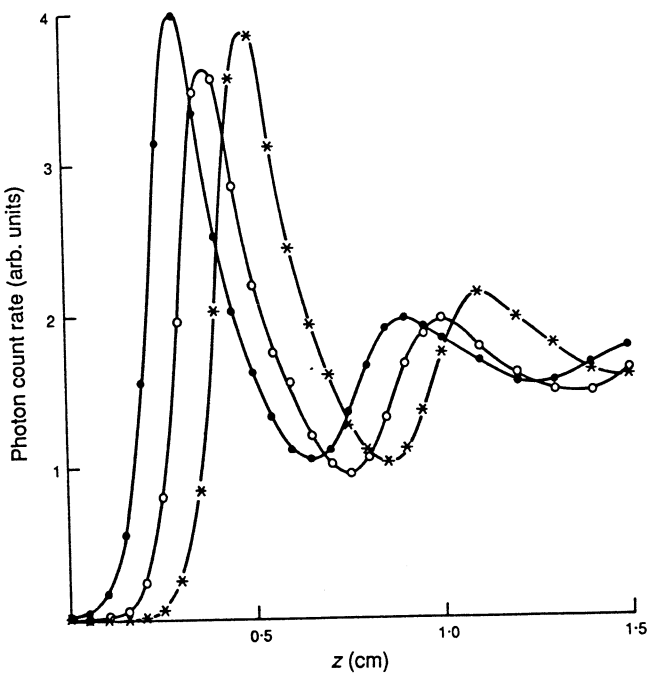

Fig. 2. Axial variation in second positive emission detected at 337·1 nm for $E/N = 331$ Td, $E = 15\ \mathrm{V\,cm^{-1}}$. The electrons were injected into the gap after acceleration through the potentials: 6·5 V, stars; 8·0 V, open circles; 9·5 V, closed circles.

Narrow band-pass filters ($\lambda_0 = 338 \cdot 0$ nm, $\Delta\lambda = 2 \cdot 5$ nm; $\lambda_0 = 391 \cdot 5$ nm, $\Delta\lambda = 3 \cdot 5$ nm) were employed to observe the radiation from the second positive system $C^3\Pi_u \rightarrow B^3\Pi_g(0,0)$ transition at 337·1 nm and from the first negative transition $B^2\Sigma_u^+ \rightarrow X^2\Sigma_g^+(0,0)$ at 391·4 nm. The $C^3\Pi_u$ state has a threshold of 11·03 eV, the $B^2\Sigma_u^+$ state 18·75 eV, and hence electrons were accelerated into the drift space by voltages varied below these thresholds. At ~3 eV the vibrational ground state cross sections represent a significant proportion of the total cross section, while above 4·5 eV they are negligible (Taniguchi *et al.* 1978). The effect of these low energy processes is to disrupt the almost linear dependence of electron energy with distance travelled in the

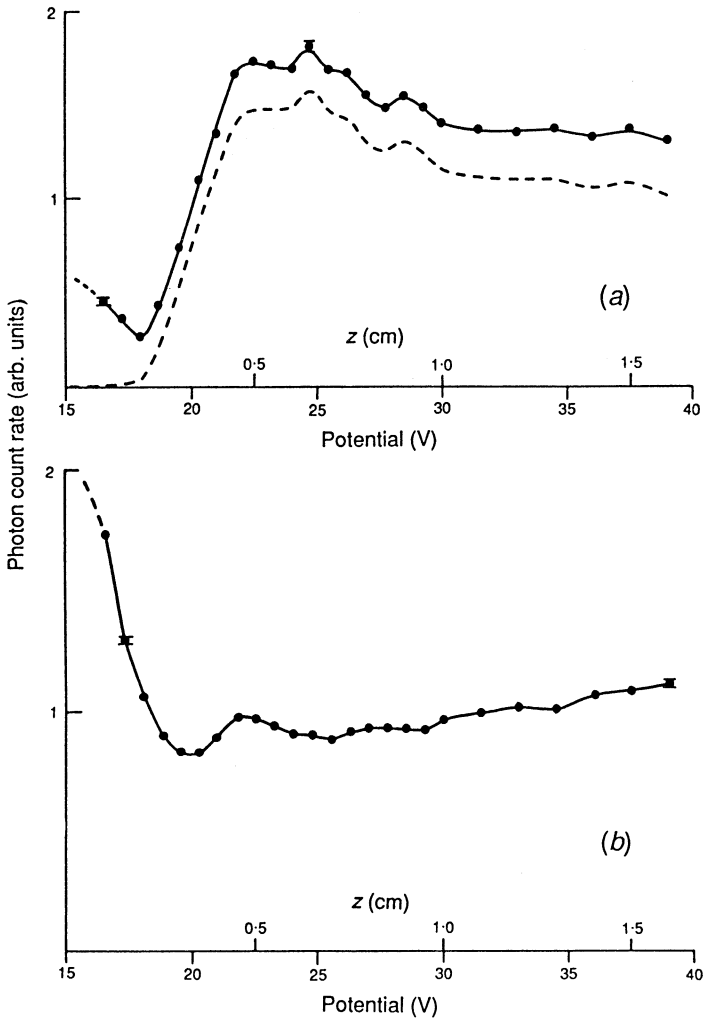

Fig. 3. Emitted radiation as a function of the total potential fallen through for $E/N = 331$ Td. The initial acceleration potential was 15 V. The detected first negative radiation (*a*) at 391·4 nm is shown by the solid points, while the dashed curve is the predicted first negative emission after subtraction of the contribution from the second positive emission. The second positive band at 337·1 nm is shown in (*b*).

field, i.e. potential difference moved through, before the electronic states are reached. Hence, by injecting quasi-mono-energetic electrons into the drift tube with energies above 5 eV, but below the threshold for electronic excitation, structure similar to the Holst–Oosterhuis layers may then be observable.

The second positive emission at 337·1 nm from a steady-state Townsend discharge in N_2 for $E/N = 331$ Td (1 Td $\equiv 10^{-17}$ V cm^2), at a pressure of 0·14 Torr and a constant anode current of 100 nA is shown in Fig. 2. In general, statistical counting uncertainties in the present experimental data are comparable with the size of the experimental points plotted on the relevant figures. Where this is not the case representative error bars are shown. The detected radiation is plotted as a function of the axial position when different acceleration potentials are used to inject the electrons. When the acceleration potential is varied, the observed peaks in the luminosity are translated in the z direction such that the first peak occurs at an axial position where the total potential difference fallen through (including the acceleration potential) is approximately 14 V. This potential corresponds closely to the maximum of the $C^3\Pi_u$ excitation cross section, indicating that this luminosity is produced by electrons which have not previously suffered any inelastic collisions.

Observations of the radiation emitted at 391·4 nm due to the $N_2^+ : B^2\Sigma_u^+ \rightarrow X^2\Sigma_g^+(0,0)$ transition are shown in Fig. 3*a*. Conditions chosen for these measurements were the same as those of Fig. 2, except that an acceleration potential of 15 V was used. Radiation detected at energies below the $B^2\Sigma_u^+$ excitation threshold (18·75 eV) displayed a similar spatial variation to the 337·1 nm radiation when measured under identical conditions, as shown in Fig. 3*b*. This has been attributed to the radiation produced at 394·3 nm due to the $N_2 : C^3\Pi_u \rightarrow B^3\Pi_g(2,5)$ transition, which is within the bandwidth of the 391·4 nm filter. Assuming that the 394·3 nm radiation has the same spatial dependence as the 337·1 nm, it is possible to determine for all positions the

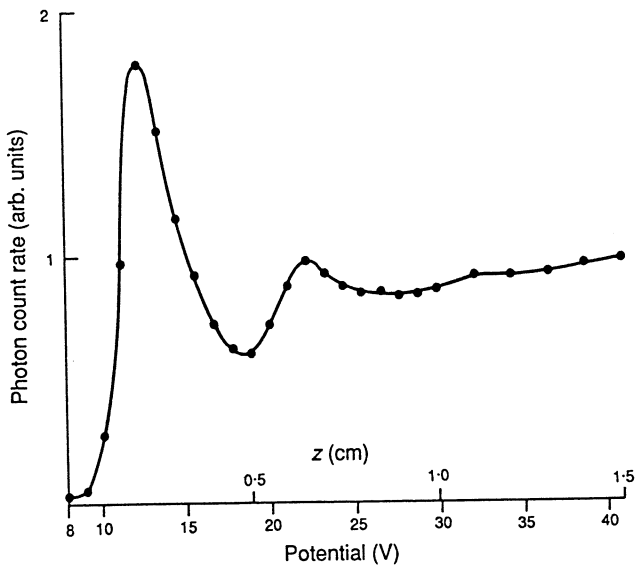

Fig. 4. Variation in 337·1 nm radiation for $E/N = 555$ Td and an initial electron acceleration potential of 8·0 V.

percentage of the total radiation detected due only to the decay of the $B^2\Sigma_u^+$ state of N_2^+. This was achieved by subtracting from the 391·4 nm bandpass count rate data the appropriate proportion of the 337·1 nm signal. This proportion is given by the ratio N(391 nm)/N(337 nm) at 0·1 cm, or equivalently when a total potential of 16·5 V is reached. The modified photon count rate at 391·4 nm which represents only the radiation due to the decay of the $B^2\Sigma_u^+$ state is indicated by the dashed curve in Fig. 3*a* and exhibits a definite threshold at approximately 19 eV as expected. Similar behaviour of the second positive and first negative emissions was observed for E/N values from 221 to 555 Td. An example of the 337·1 nm radiation for $E/N = 555$ Td and an acceleration potential of 8 V is shown in Fig. 4.

3. Monte Carlo Simulation

Monte Carlo simulation studies provide a convenient and informative way of analysing the type of experiments described here. The method used in this simulation of the experiments was based on a 'null-collision' Monte Carlo method (Skullerud 1968; Braglia 1985). The computer code was tested by using the Reid (1979) ramp model as a benchmark (Brennan 1986). The cross sections used in the nitrogen simulation were set C from Tagashira *et al.* (1980), but modified to include an excitation to the $B^2\Sigma_u^+$ state of N_2^+ (Stanton and St. John 1969) and a dissociative ionisation cross section (E. E. Kunnhardt, personal communication 1983). This allowed a comparison with the experimental investigation of the cathode non-equilibrium region. The triplet state cross sections of Cartwright *et al.* (1977), adopted by Tagashira *et al.* (1980), were modelled by an exponential decay above 50 eV in the current work.

It should be noted that isotropic scattering was assumed in all channels, both elastic and inelastic, and that all electronic excitations were modelled by an excitation to the lowest vibrational level, with an energy loss equal to the threshold of that level. In order to simulate the production of electrons in the experiment, electrons were given an initial energy at the cathode which included an exponentially decaying source with a 1/e width of 0·1 eV. Typically, of the order of 10^5 electrons were released from the cathode surface which was assumed to be totally reflecting. The results have been obtained with an energy resolution of 0·1 eV and a spatial resolution of 1% of the drift gap separation.

Fig. 5 shows the simulation results constructed as a histogram of the production of $C^3\Pi_u$ excitations as a function of the potential accelerated through for 8 eV initial electron energy. The qualitative similarity between the experimental (Fig. 2) and simulated data is apparent. The fluctuating photon count rate can be explained by following the electron energy distribution function obtained from the Monte Carlo simulation. Fig. 6*a* shows the energy distribution for those electrons which have fallen through 10·0–10·5 V for $E/N = 330$ Td. The high energy group is indicative of the number of electrons which have moved through the gap suffering only elastic collisions. The next highest energy group has lost ~6 eV and it represents those electrons which have suffered one inelastic collision resulting in the excitation of the molecule to the $A^3\Sigma_u^+$ electronic level (threshold energy 6·17 eV). Similarly, the

next few groups in the energy distribution represent energy losses between 6 and 11 eV due to excitation of other higher lying electronic states. The gap between 5 and 10 eV in the energy distribution function follows since vibrational excitation of the ground state is not possible for electrons in this range, due to the initial 8 eV injection energy.

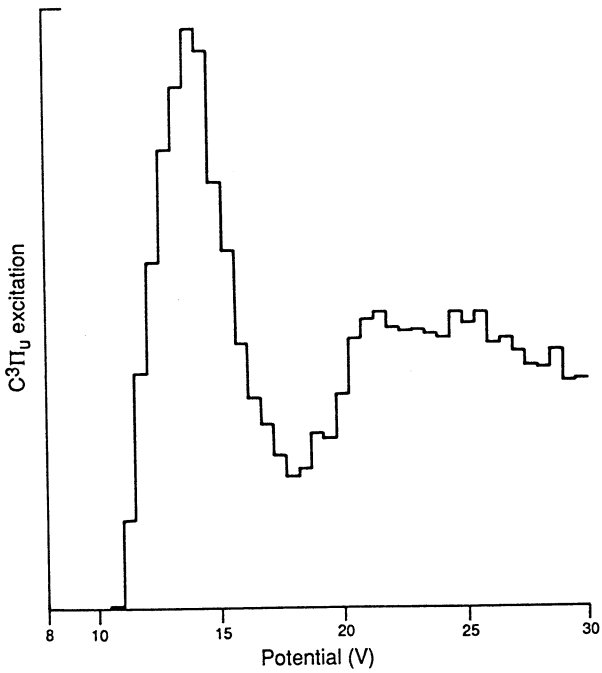

Fig. 5. Monte Carlo simulation of $C^3\Pi_u$ state excitation for $E/N = 330$ Td. The electrons were started at the cathode with an energy of 8 eV.

The energy distribution after the electrons have fallen through 20·2–20·7 V is given in Fig. 6*b*. At this stage far fewer electrons have moved through the gap without suffering any inelastic collisions and the remaining groups have been dispersed by inelastic collisions resulting in the production of various excited states. The electron energies are more widely distributed over the range due to the large number of collisions that have occurred; however, the non-equilibrium in the distribution function is still evident.

The peaks in the radiation at 337·1 nm arise when the different groups of electrons in the distribution function have energies near the maximum in the cross section for excitation of the $C^3\Pi_u$ state, which is relatively sharply peaked at ~14 eV. As electrons move further through the gas and experience more collisions, the situation increases in complexity and the electron energies become more evenly distributed over the energy range. Hence, the peaks in luminosity rapidly disappear, and the electron energy distribution evolves towards equilibrium.

Monte Carlo simulation results for excitation of the $B^2\Sigma_u^+$ and $C^3\Pi_u$ states are presented in Fig. 7 for $E/N = 330$ Td and a simulated acceleration potential

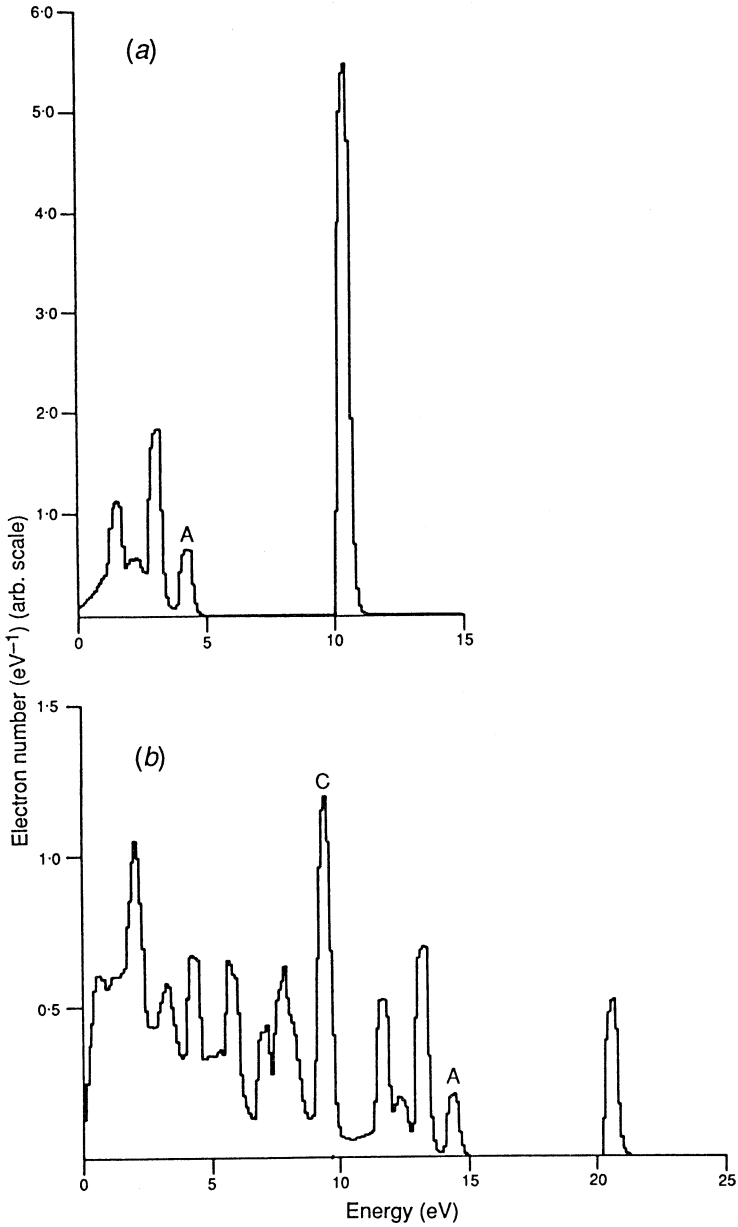

Fig. 6. Electron energy distribution from the Monte Carlo simulation ($E/N = 330$ Td) once the electrons have fallen through a potential difference of (*a*) 10·0–10·5 V and (*b*) 20·2–20·7 V. The peaks labelled A and C arise from excitation of the $A^3\Sigma_u^+$ and $C^3\Pi_u$ states respectively. The initial electron energy was 8 eV.

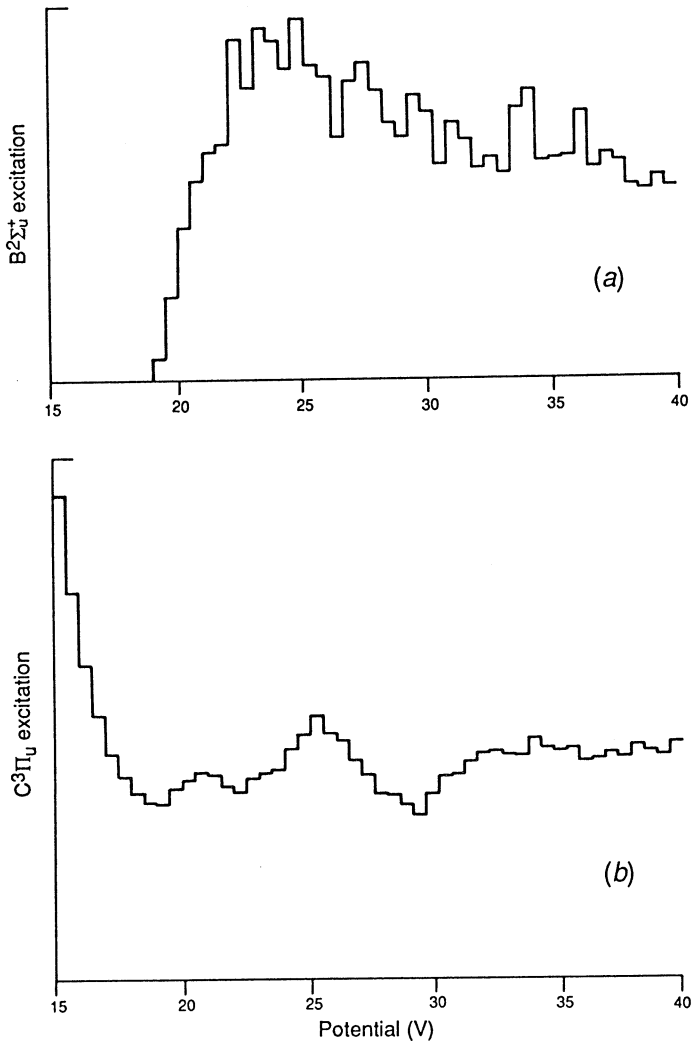

Fig. 7. Monte Carlo simulation results for (*a*) the $B^2\Sigma_u^+$ state and (*b*) the $C^3\Pi_u$ state excitation. In each case $E/N = 330$ Td and the initial electron energy was 15 eV.

of 15 V. The qualitative agreement between the simulation results and the experimental photon count rates (Fig. 3) is apparent. The electron energy distribution function after the electrons have moved through 19·6–20·1 V is presented in Fig. 8*a*. A large group of electrons can excite the $B^2\Sigma_u^+$ state and it is this group of electrons which produces the peak in the radiation at 391·4 nm. It is possible to clearly recognise those electrons in the energy distribution which have suffered inelastic collisions resulting in excitations of the ground state molecule to the $C^3\Pi_u$ and $A^3\Sigma_u^+$ states. Fig. 8*b* shows the distribution of electron energies after they have fallen through 24·7–25·2 V. Although the $B^2\Sigma_u^+$ excitation cross section is a monotonically increasing function of

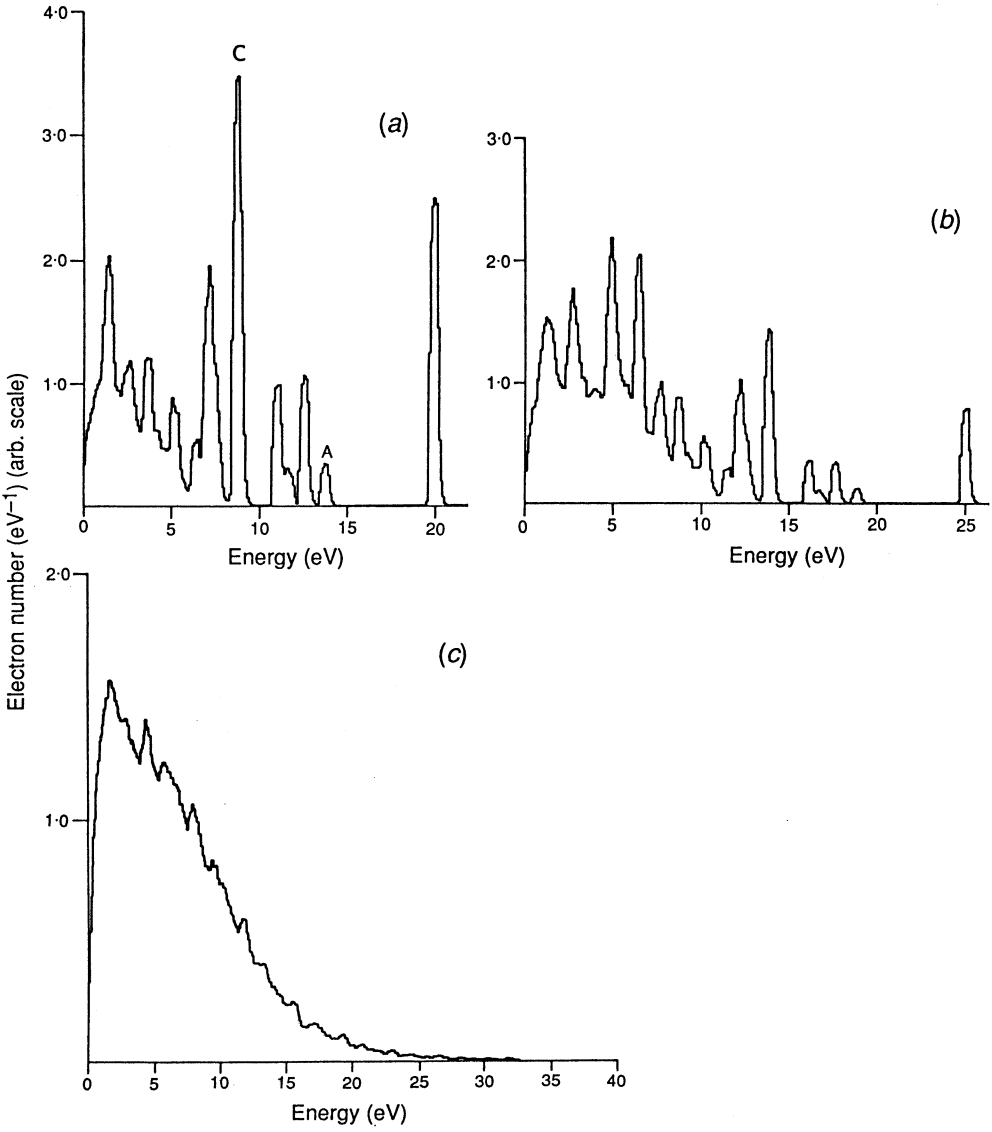

Fig. 8. Evolution of the electron energy distribution function for $E/N = 330$ Td and an initial electron energy of 15 eV. In (*a*) the large number of electrons with 9 eV have suffered one inelastic collision resulting in $C^3\Pi_u$ state excitation. In (*b*) relatively few electrons remain which have not suffered an inelastic collision. The distribution function in (*c*), after the electrons have fallen through 35·2–35·7 V, shows the approach to equilibrium.

energy, for the energy range important in this simulation, the light output decreases with increasing distance due to the depletion of the high energy group. The energy distribution function has rapidly increased in complexity due to excitation of lower energy levels and approaches the steady state in Fig. 8*c*.

Simulation results for $E/N = 550$ Td and 8 eV initial electron energy are shown in Fig. 9 and clearly reproduce the general features of the experiment

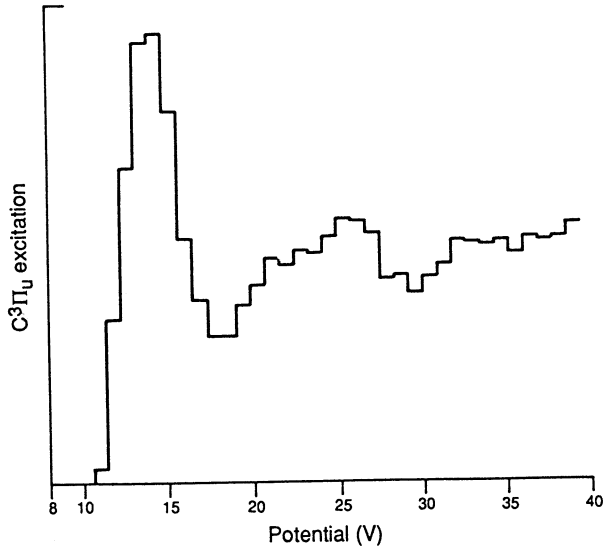

Fig. 9. Simulation of the $C^3\Pi_u$ state excitation for $E/N = 550$ Td. The initial electron energy was 8 eV.

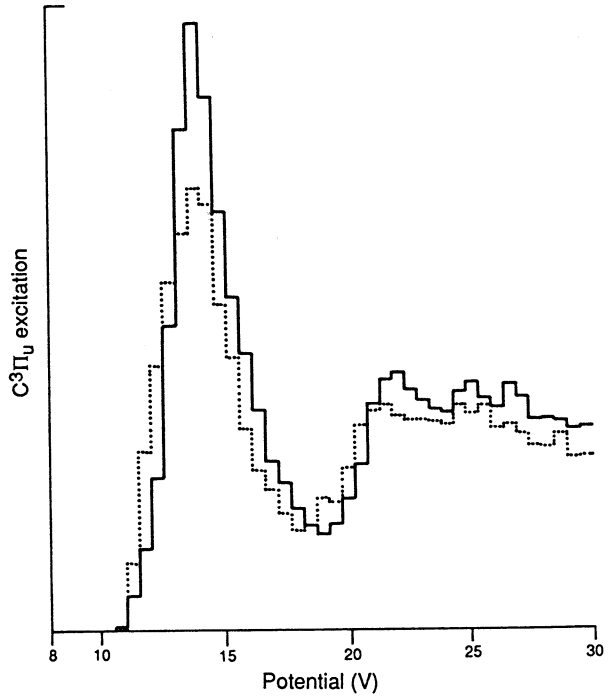

Fig. 10. Comparison of $C^3\Pi_u$ state excitation at 330 Td using two cross-section data sets: dotted line, Tagashira *et al.* (1980); solid line, Phelps and Pitchford (1985).

at the higher E/N value. However, despite the good qualitative agreement between simulation and experiment, with all the results presented there are some important quantitative discrepancies which will now be discussed.

Clearly, there are differences which cannot be explained by the spatial resolution of the detection system, contact potentials or statistical fluctuations in the experiment or simulation. In particular, for $E/N = 330$ Td the heights of the initial peak and subsequent trough in the experimental data (Fig. 2) differ from the simulation data (Fig. 5). The ratio of this peak-to-trough in the experimental data is $3 \cdot 68 \pm 0 \cdot 05$, whereas the simulation has the larger ratio of $4 \cdot 25$. Note that the simulation peak-to-trough ratio has been calculated from the electron energy distribution functions and hence the statistical error is negligible. For $E/N = 555$ Td the comparison of the peak-to-trough ratios agrees more favourably, with a ratio of $2 \cdot 99 \pm 0 \cdot 04$ for the experimental data and $3 \cdot 13$ for the simulation. Our results indicate that either too many electrons reach the threshold of the $C^3\Pi_u$ state without inelastic collision or the magnitude of the $C^3\Pi_u$ cross section is too large.

Given this discrepancy between the Tagashira *et al.* (1980) model of nitrogen and the experimental results it was decided to adopt a different cross-section set. The cross sections chosen were those of Table 1 in Phelps and Pitchford (1985). Again the data were modified to include excitation to the $B^2\Sigma_u^+$ state. Using these cross sections the simulation of the cathode non-equilibrium region was repeated. The excitation rate histogram for the $C^3\Pi_u$ state at $E/N = 330$ Td, for an injection energy of 8 eV and derived from the Phelps–Pitchford model of nitrogen, is presented in Fig. 10 (solid line), and compared with the previous results obtained with the model of Tagashira *et al.* (dotted line). The use of the Phelps–Pitchford set of collision cross sections in the simulation again predicts the qualitative nature of the luminosity at $337 \cdot 1$ nm. The initial peak-to-trough ratio in the excitation rate for the Phelps–Pitchford model is $6 \cdot 03$. This can be compared with the value of $4 \cdot 25$ for the Tagashira *et al.* model and the experimental result of $3 \cdot 68$. The height of the initial peak in the Phelps–Pitchford model suggests that the $C^3\Pi_u$ cross section employed by them is too large. This has been confirmed by recent electron beam measurements (P. J. O. Teubner and M. J. Brunger, personal communication 1988). Furthermore, Jelenkovic and Phelps (1987) in reference 15 of their paper, stated that a noticeable improvement in the agreement between calculated and measured spatial ionisation and $C^3\Pi_u$ excitation coefficients is obtained when the $C^3\Pi_u$ cross section of the Phelps–Pitchford set is reduced by 33%.

4. Conclusions

Experiments in the cathode non-equilibrium region of a steady-state Townsend discharge of the type reported in this paper could clearly play an important role in the evaluation of cross-section data. The current experimental results suggest that the assumed sets of cross sections of both Tagashira *et al.* (1980) and Phelps and Pitchford (1985) require modification. Both models predict greater excitation of the $C^3\Pi_u$ state in the first peak than that observed experimentally. Reduction of the magnitude of the $C^3\Pi_u$ state excitation cross section, or alternatively, an increase in the strengths of some of the smaller energy loss processes would improve agreement between simulation

and experiment. Given the large number of free parameters in a cross-section set, such as size and energy dependence of each cross section, the uniqueness of any alterations to improve agreement with experiment is questionable. However, by investigating the radiation from the decay of a number of excited states with a range of excitation thresholds, different parts of the distribution function could be probed. For example, quenching the metastable $A^3\Sigma_u^+$ state (threshold at 6·17 eV) would yield information about the lower energy region of the distribution and in particular the appropriateness of the cross section for this state. It is evident that additional studies of the type discussed here would be useful. A chosen set of cross sections should not only yield quantitative agreement between experimental and theoretical equilibrium transport parameters, but should also describe measurements in the non-equilibrium regions of the discharge.

Acknowledgments

The authors are indebted to Professor H. A. Blevin for his valuable contributions during the course of this work. We also wish to thank Dr P. J. O. Teubner and Dr M. J. Brunger for useful discussions. L.J.K. wishes to acknowledge the support of a Zonta International Amelia Earhart Fellowship Award and M.J.B. that of a Flinders University Research Scholarship.

This work was support by funds from the Australian Research Council and the Flinders University Research Budget.

References

Blevin, H. A. (1985). Seventeenth Int. Conf. on Phenomena in Ionised Gases, Budapest 1985 (Eds J. S. Bakos and Z. S. Uzsa Sörlei), p. 308.
Boeuf, J. P., and Marode, E. (1984). *J. Phys.* D **17**, 1133.
Braglia, G. L. (1985). *Contrib. Plasma Phys.* **25**, 567.
Brennan, M. J. (1986). Ph.D. Thesis, Flinders University of South Australia (unpublished).
Cartwright, D. C., Trajmar, S., Chutjian, A., and Williams, W. (1977). *Phys. Rev.* A **16**, 1041.
Druyvesteyn, M. (1932). *Z. Phys.* **73**, 33.
Fletcher, J. (1985). *J. Phys.* D **18**, 221.
Holst, G., and Oosterhuis, E. (1921). *Physica* **1**, 78.
Jelenkovic, B. M., and Phelps, A. V. (1987). *Phys. Rev.* A **36**, 5310.
Phelps, A. V., and Pitchford, L. C. (1985). JILA Information Center Report No. 26.
Reid, I. D. (1979). *Aust. J. Phys.* **32**, 231.
Skullerud, H. R. (1968). *J. Phys.* D **1**, 1567.
Stanton, P. N., and St. John, R. M. (1969). *J. Opt. Soc. Amer.* **59**, 252.
Tagashira, H., Taniguchi, T., and Sakai, Y. (1980). *J. Phys.* D **13**, 235.
Taniguchi, T., Tagashira, H., and Sakai, Y. (1978). *J. Phys.* D **11**, 1757.
Wedding, A. B., Blevin, H. A., and Fletcher, J. (1985). *J. Phys.* D **18**, 2351.
Wedding, A. B., and Kelly, L. J. (1989). *Aust. J. Phys.* **42**, 101.

Manuscript received 20 February, accepted 11 April 1989